

# Shapes of agglomerates in plasma etching reactors

Fred Y. Huang<sup>a)</sup> and Mark J. Kushner<sup>b)</sup>

University of Illinois, Department of Electrical and Computer Engineering, 1406 West Green Street, Urbana, Illinois 61801

(Received 18 November 1996; accepted for publication 21 January 1997)

Dust particle contamination of wafers in reactive ion etching (RIE) plasma tools is a continuing concern in the microelectronics industry. It is common to find that particles collected on surfaces or downstream of the etch chamber are agglomerates of smaller monodisperse spherical particles. The shapes of the agglomerates vary from compact, high fractal dimension structures to filamentary, low fractal dimension structures. These shapes are important with respect to the transport of particles in RIE tools under the influence electrostatic and ion drag forces, and the possible generation of polarization forces. A molecular dynamics simulation has been developed to investigate the shapes of agglomerates in plasma etching reactors. We find that filamentary, low fractal dimension structures are generally produced by smaller ( $<100$ s nm) particles in low powered plasmas where the kinetic energy of primary particles is insufficient to overcome the larger Coulomb repulsion of a compact agglomerate. This is analogous to the diffusive regime in neutral agglomeration. Large particles in high powered plasmas generally produce compact agglomerates of high fractal dimension, analogous to ballistic agglomeration of neutrals. © 1997 American Institute of Physics. [S0021-8979(97)01709-X]

## I. INTRODUCTION

Particle contamination is a continuing concern in plasma processing discharges as used for semiconductor device manufacturing.<sup>1</sup> These discharges are typically low gas pressure devices (tens to hundreds of mTorr) which operate with electron densities of  $10^9$ – $10^{11}$   $\text{cm}^{-3}$ . The typical sizes of contaminating particles are 100s nm to a few microns. With the advent of submicron feature sizes in microelectronics devices, dust contamination by even the smaller particles may result in a killer defect. Therefore, controlling the generation and transport of particles in plasma processing discharges is of great interest to the semiconductor manufacturing community.

The fundamentals of transport and trapping of particles in low pressure plasmas have been studied by several authors.<sup>2–6</sup> Briefly, dust particles negatively charge in plasmas, and so are subject to both mechanical and electrical forces. The dominant forces responsible for particle transport are ion drag, electrostatic, neutral drag, thermophoretic, gravitational, and self-diffusion. Ion drag forces, which result from long range Coulomb interaction between ions and the negatively charged particle, accelerate particles in the direction of the net ion flux, typically towards the boundaries of the reactor. Electrostatic forces accelerate particles towards the maximum in the plasma potential, typically near the center of the plasma. Fluid drag accelerates particles in the direction of bulk gas flow. The characteristic trapping of dust particles often observed at the sheath edges<sup>1</sup> results from an equilibrium between the oppositely directed ion drag and electrostatic forces.

Particles which are collected on surfaces in plasma etching tools or downstream of the plasma chamber are often

clusters or agglomerates of smaller, monodisperse “primary” spherical particles.<sup>7–9</sup> These observations imply that primary particles grow to a terminal size before agglomerating to form these larger structures. The agglomeration process is problematic since the dust particles are charged negative. This requires the reactants in an agglomerating collision to have sufficient kinetic energy to overcome the mutual electrostatic repulsion. For example, the agglomeration of two 1  $\mu\text{m}$  radius Si dust particles having 5000 elementary charges each requires center of mass speeds of  $> 1$   $\text{m s}^{-1}$ . It has been found that collected agglomerates typically also have different morphologies. Agglomerates which are made of small ( $<100$ s nm) primary particles tend to be dendritic and have a small fractal dimension. Agglomerates made of large ( $>\mu\text{ms}$ ) primary particles tend to be compact and have a large fractal dimension.

In a previous publication, we discussed results from a model for dust particle agglomeration called the particle agglomeration model (PAM) in which we derived scaling laws for the growth of agglomerates from primary particles.<sup>10</sup> We found that agglomeration is more likely for larger particles and higher plasma powers, which produce larger ion drag forces. Due to the scaling of the charging and acceleration of particles with particle size, these conditions result in primary particles having sufficiently large kinetic energies to overcome their mutual electrostatic repulsion and produce agglomerates. We also found that the growth of agglomerates depends on the shape of the particle. In cases where we forced agglomerates to be spherical, the rate of agglomeration was low and the terminal agglomerate size was small. If agglomerates are spherical, an approaching primary particle experiences electrostatic repulsion from the full charge of the agglomerate. Hence, primary particles of a given speed are eventually unable to overcome the Coulomb barrier as the agglomerate grows. In our study, agglomerates which were allowed to have cylindrical shapes evolved into high aspect

<sup>a)</sup>Electronic mail: f-huang@uiuc.edu

<sup>b)</sup>Electronic mail: mjk@uiuc.edu

ratio (long and narrow) structures. An agglomerate which has such an aspect ratio has its charge distributed over a distance of many primary particle radii. The Coulomb force on the primary particle is proportionally lower and therefore low speed primary particles can add to the agglomerate. If agglomerates grow to sizes approaching or exceeding the linearized Debye length, some charge on the agglomerate may be shielded from the primary particle during its approach, thereby leading to additional growth.

These scaling laws, and the cited experimental observations of agglomerate shapes, imply that the shape and growth of agglomerates depend on the size, speed, and previous history of the agglomerate. To investigate these processes, we have improved upon the PAM by developing a molecular dynamics (MD) model for the agglomeration of particles in low temperature plasmas. The MD-PAM simulates the interaction of individual charged primary particles with a growing agglomerate of arbitrary shape while considering electrostatic shielding. We found that particles which have kinetic energy marginally able to broach the Coulomb repulsion barrier generate agglomerates which are dendritic and have low fractal dimension. These agglomerates resemble neutral aerosols which grow in a diffusive or random walk regime, and tend to be composed of smaller primary particles (<100s nm). Particles which have large kinetic energies which are sufficient to broach the Coulomb barrier form compact agglomerates of high fractal dimension, which resemble neutral agglomerates grown in a ballistic regime. These agglomerates tend to be composed of larger primary particles (>100s nm). The MD-PAM will be described in Sec. II followed by a discussion of our parametric investigation of particle agglomeration in plasmas in Sec. III. Our concluding remarks are in Sec. IV.

## II. DESCRIPTION OF THE MODEL

The MD-PAM uses molecular dynamics techniques to build agglomerates on a particle-by-particle basis. In the results discussed here, the MD-PAM is not executed within the framework of a reactor scale particle transport mode, as is the previously described PAM, although particle velocity distributions from the reactor scale simulation are used. The purpose of the MD-PAM is to investigate the processes leading to classes of agglomerate shapes in plasma processing reactors, and so we address only those phenomena here. The general procedure followed in the MD-PAM is as follows.

We begin by specifying electron and ion densities and their temperatures, and the radius and mass density of the primary dust particles. Given these parameters, the equilibrium electrical charge on the dust particles is computed as described in Ref. 11. Initial velocity vectors are then chosen for each of the two reactant particles (either two primary particles, a primary particle and an agglomerate, or two agglomerates). An impact location is chosen and the particles are “backed off,” following the reverse trajectories of their initial velocity vectors to locations where the repulsive electrical potential between the particles is < 1% of its value when the particles touch. An impact parameter is randomly chosen between zero and the sum of the radii of the two particles. The trajectories of the particles are then integrated

forward in time while considering the plasma shielded electrical force between them using a third order Runge–Kutta technique having an adaptive time step. If the particles collide, an agglomerate is formed consisting of the two particles. If the particles do not collide, the process is repeated choosing different initial velocities and/or different impact parameters. If an agglomeration does not occur after a specified number of trials (typically 5000), we declare that these particular plasma conditions (ion density, electron temperature, particle size, particle mass density, initial velocity) will not produce a larger agglomerate. We do not resolve the mechanical forces which bind primary particles into an agglomerate. Once a collision occurs and a primary particle is added to an agglomerate, we assume that the coordinates of all primary particles are fixed with respect to the center of mass of the agglomerate. That is, we assume a rigid body for the agglomerate.

We typically begin with two primary (monomer) particles and build the agglomerate by adding additional monomer particles. The orientation of the agglomerate is important in determining the propensity for agglomeration since the incident primary particle experiences a different force depending on the local morphology. To account for this dependency, Eulerian angles are randomly chosen for the agglomerate. After backing off the particles, the coordinates of the agglomerate are rotated about Cartesian axes based on the Eulerian angles with an origin at the center of mass of the agglomerate. The trajectories of the agglomerate and monomer are then integrated forward in time.

An important process in the agglomeration of particles in plasmas is the shielding of charge on larger agglomerates. If the size of the agglomerate is commensurate with the shielding length, which for our conditions is the linearized Debye length,<sup>12</sup> a primary particle approaching one end of the agglomerate may not “see” the charge at the other end of the agglomerate. Precise representation of this shielding requires a dynamic three-dimensional solution of Poisson’s equation with accounting of electron and ion motion, an exercise which is beyond the scope of this work. We approximate the effects of plasma shielding by using an effective charge  $Q'(r_{ij})$  in the force equation for the colliding particles, where  $r_{ij}$  is the distance between primary particles of the agglomerate. For example, the force on the incident primary particle is

$$f_j = \frac{1}{4\pi\epsilon_0} \sum_i \frac{Q_j Q'_i(r_{ij})}{r_{ij}^2}, \quad r_{ij} = |\mathbf{r}_i - \mathbf{r}_j|, \quad (1a)$$

$$Q'_i(r_{ij}) = Q_i \left( 1 - \frac{\int_R^{r_{ij}} 4\pi r^2 \exp(-r/\lambda) dr}{\int_R^\infty 4\pi r^2 \exp(-r/\lambda) dr} \right), \quad (1b)$$

where  $R$  is the radius of the primary particle,  $\lambda$  is the shielding distance,  $Q_i$  is the unshielded charge, and the sum is over primary particles in the agglomerate. The effective charge reduces the repulsion between the incident primary particle, and primary particles in the agglomerate further than  $\lambda$  away due to the intervening plasma shielding. In doing so, the effective charge of primary particles at the opposite end of a “chainlike” agglomerate is small.

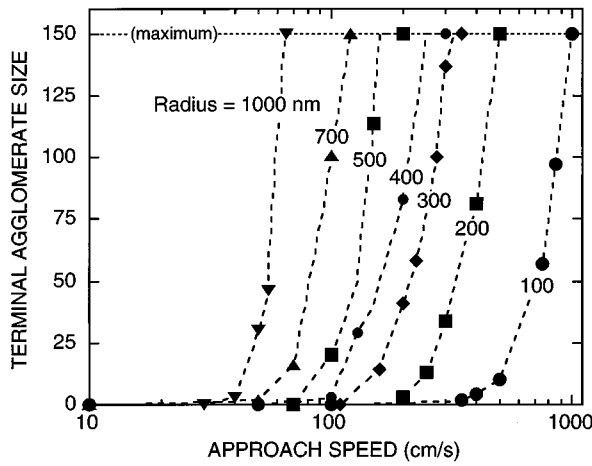


FIG. 1. Maximum agglomerate size (in units of primary particles/agglomerate) for specified approach velocities (cm/s) and primary sizes (nm). With the increased kinetic energy at higher velocities and primary particle size, particles can produce larger agglomerate structures.

In our previous work, we found that the kinetic energy of the reactants in large part determines the terminal agglomeration size. The MD-PAM is not fully integrated into a plasma model, and so estimates of the initial velocities of the reactants are required. These values are obtained from a plasma equipment model into which dust particle transport is fully integrated. (This model is described in Refs. 3 and 13.) The integrated particle transport model is executed for the conditions of interest and the velocity distributions of the dust particles are calculated. The velocity distribution provides us with realistic upper limits for our parametric studies.

### III. AGGLOMERATION SHAPES

In this section, we will discuss shapes of agglomerates for various plasma reactor conditions and particle sizes. For the first results, we have specified the electron and ion temperatures as 1.0 and 0.05 eV, respectively, and a particle composition of Si (mass density  $2.33 \text{ g cm}^{-3}$ ). For these conditions, particles having radii of 100, 300, and 1000 nm particles have charges of  $-215$ ,  $-654$ , and  $-2277q$ . The agglomerate (or larger collision partner) is initially at rest, as it would be if residing in a trap, and we specify the speed of the monomer primary particle. The maximum number of trials to add an additional monomer to an agglomerate is 5000. We stopped building the agglomerate when it contained 150 primary particles. It has been our experience that particles which reach this size will generally continue to grow.

The terminal agglomerate size (expressed as the number of primary particles in the agglomerate) is shown in Fig. 1 as a function of the incident speed of the monomer for particle radii of 100 nm to  $1 \mu\text{m}$ . The terminal agglomerate size increases with speed and, for a fixed speed, increases with primary particle size. This scaling follows from the requirement that monomer particles must have sufficient kinetic energy to overcome the repulsive Coulomb barrier of the larger agglomerate. The charge on particles of radius  $R$  scales as

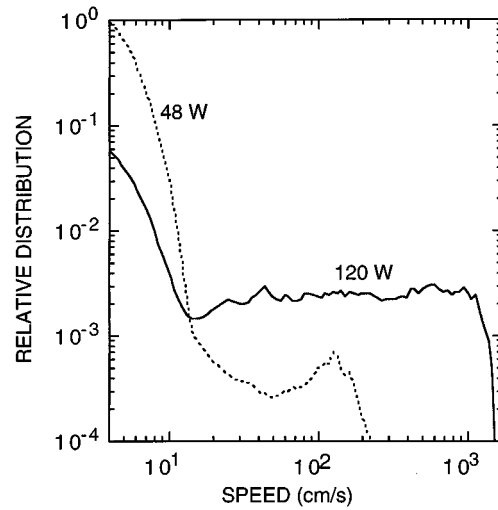


FIG. 2. Velocity distributions for 100 nm primary particles in a 100 mTorr Ar discharge for different powers: 48 and 120 W. While the majority of the primary particles are at low speeds (a few 10s cm/s), particles can reach several hundreds of cm/s entering the sheath.

$Q \sim CT_e \sim RT_e$ , where  $T_e$  is the electron temperature, and  $C$  is the capacitance of the particle. The lab energy required for an agglomeration therefore scales as

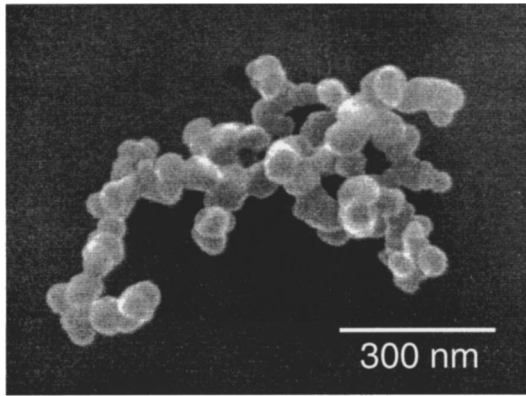
$$E = \frac{1}{2} M_1 V_1^2 \sim \frac{Q_1 Q_2}{R_1 + R_2} \sim \frac{R_1 R_2 T_e^2}{R_1 + R_2}, \quad (2)$$

and so the required speed of the primary particle to undergo agglomeration scales as

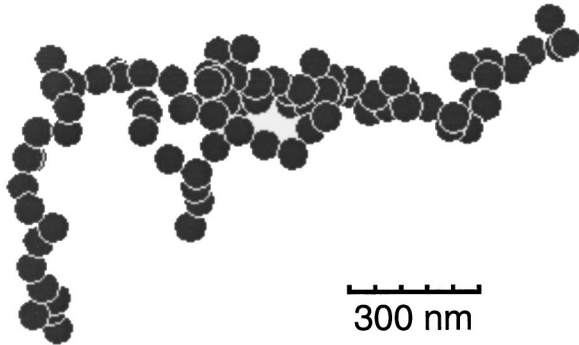
$$V_1 \sim \left( \frac{R_2}{R_1^2 (R_1 + R_2)} \right)^{1/2} T_e. \quad (3)$$

As shown in Fig. 1, agglomeration requires relative speeds of 10s to 100s cm/s for typical sizes of particles. Although the majority of particles in RIE discharges do not have these speeds, particles in the tail of the velocity distribution can broach the critical speed for agglomeration. For example, typical particle velocity distributions for 100 nm monomer particles are shown in Fig. 2 for a RIE discharge operated in 100 mTorr of Ar at 48 and 120 W. These distributions were computed with the dust transport simulation (DTS) described in Ref. 13. Although the bulk of the particles have low average speeds (a few to 10s cm/s), the maximum particle speeds are 100s cm/s to as large as 1000 cm/s. The maximum particle speed increases with increasing power which increases ion drag forces. Particle agglomeration in plasmas is therefore not a process in which all particles participate, but rather particles which populate the tail of the velocity distribution.

A scanning electron micrograph of a typical dust particle collected from the exhaust of an RIE discharge sustained in  $SF_6$  is shown in Fig. 3(a).<sup>14</sup> The particle is an agglomerate of smaller primary particles, approximately 40 nm in diameter. A typical agglomerate generated by the MD-PAM, using silicon primary particles of approximately the same size, is shown in Fig. 3(b). The shape of the agglomerate from the MD-PAM shows good qualitative agreement with the experi-



(a)



(b)

FIG. 3. A comparison of (a) a SEM micrograph of a dust particle collected in an  $\text{SF}_6$  discharge (Ref. 14) and (b) a typical agglomerate generated by the MD-PAM under similar conditions. Both the collected and simulated particle consist of spherical primary particles roughly 40 nm in diameter, and show similar shapes.

mental data. Both agglomerates exhibit filamentary (low fractal dimension) shapes. The structure of the agglomerates, however, largely depends on the size, charge, and relative kinetic energy of the collision partners. For example, agglomerates composed of 1 micron (radius) particles having successively larger approach speeds (50, 75, 100, and 300 cm/s) for the incoming primary particle are shown in Fig. 4. We find that at low particle speeds, the shape of the agglomerate is filamentary and has a low fractal dimension, akin to the “diffusive” agglomeration regime for neutral aerosols. At high particle speeds, the agglomerate is compact and has a high fractal dimension, akin to “ballistic” agglomeration regime for neutral aerosols. At low incident speeds, the incoming particle’s kinetic energy is small compared to the potential energy of the agglomerate, and so it is scattered with a large deflection angle. Growth occurs, at best, at the periphery of the agglomerate, which results in forming filamentary, low fractal dimension shapes. These shapes are self-perpetuating since the electrostatic repulsion of a primary particle approaching the end of a chainlike agglomerate is lower than that approaching a compact agglomerate composed of the same number of primary particles. The lower potential energy results from both increased distance from

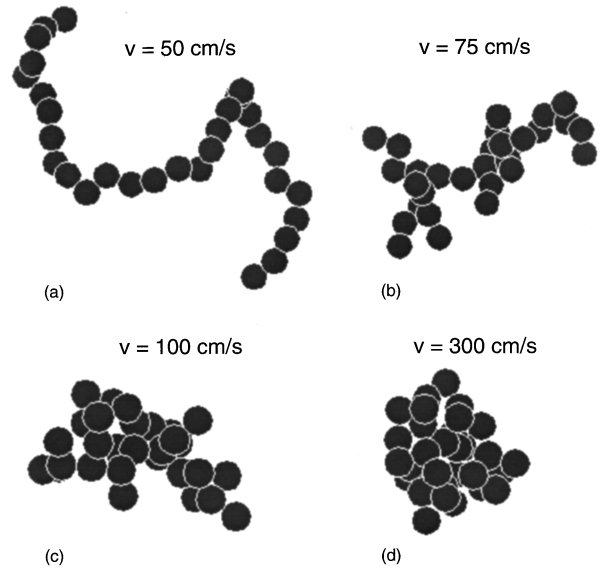


FIG. 4. Simulated agglomerates generated using 1  $\mu\text{m}$  radius particles over a range of approach velocities. (a) 50, (b) 75, (c) 100, and (d) 300 cm/s. At low speeds, the primary particles form filamentary agglomerates. At high velocities, the agglomerates form a more compact, ballistic type structure.

the other members of the agglomerate, and some amount of additional plasma shielding. As the incident speed increases, at constant particle size, the kinetic energy of the incoming particle is progressively able to overcome the electrostatic repulsion of the growing agglomerate. At sufficiently high incident velocity, agglomerate growth is essentially ballistic.

Given these observations, the shape of the agglomerate should depend on the ratio of the kinetic energy of the incoming particle to the repulsive energy,

$$\beta = \frac{\frac{1}{2} M_1 V_1^2}{\left( \frac{1}{4\pi\epsilon_0} \frac{Q_1 Q_2}{R_1 + R_2} \right)} \sim \frac{R_1^3 V_1^2 (R_1 + R_2)}{R_1 R_2 T_e^2}. \quad (4)$$

Small values of  $\beta$  correspond to small particles having low speeds approaching large agglomerates holding high charge (resulting from either their size or large electron temperature of the plasma). Under these conditions, the agglomerate should be filamentary. Large values of  $\beta$  (large particles, high velocities, and low charge states) should produce agglomerates which are compact. For example, the agglomerates shown in Fig. 4, transitioning from filamentary to compact, have normalized  $\beta$  values of 0.25, 0.56, 1.0, and 9.0. Following this reasoning, particles having approximately the same value of  $\beta$  should therefore form agglomerates having approximately the same shape. This scaling is shown in Fig. 5 where we see agglomerates generated by the MD-PAM having primary particles with radii of 100, 300, and 1000 nm, but the same value of  $\beta$  (approach speeds for the incoming primary particle of 1000, 333, and 100 cm/s). The shapes of the agglomerates are qualitatively the same.

The local conditions in the plasma play a key role in the rate of agglomeration and agglomerate shapes since the electron temperature and plasma density determine the charge state of the primary particle and the shielding length. The ion

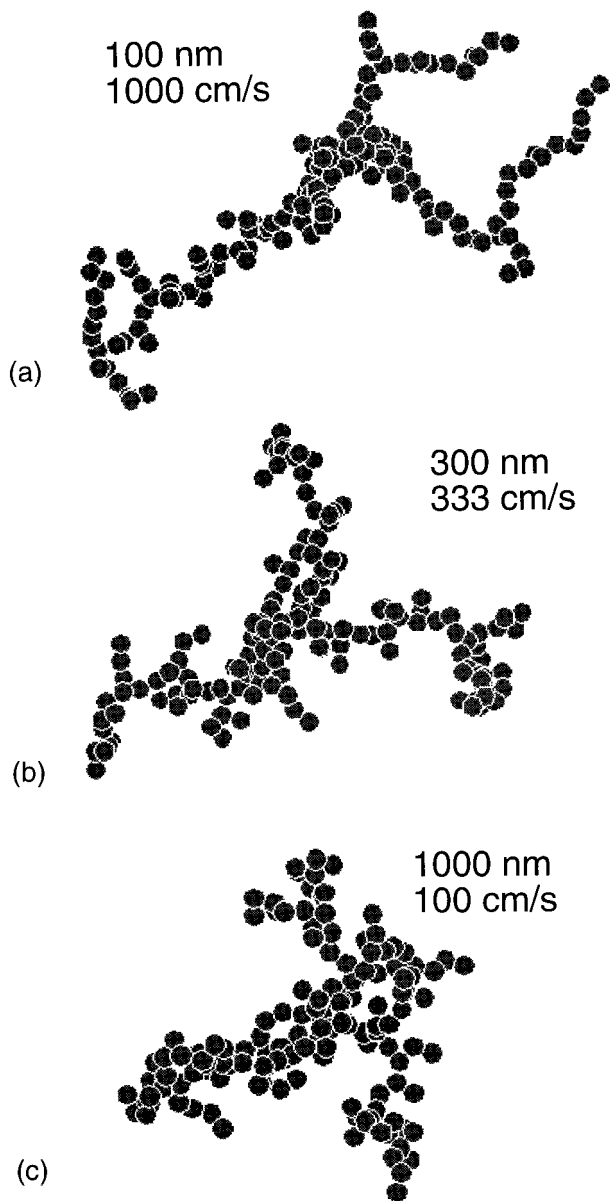


FIG. 5. Morphologies of agglomerates of the same  $\beta$  value. (a)  $R = 100$  nm,  $v = 1000$  cm/s. (b)  $R = 300$  nm,  $v = 333$  cm/s. (c)  $R = 1000$  nm,  $v = 100$  cm/s. The agglomerates qualitatively have the same, filamentary shape.

fluxes, gas flow, and plasma potential additionally determine the magnitude of acceleration of the particles. Predictions of agglomerate sizes and shapes must therefore be performed on a reactor-by-reactor basis. Using results from the MD-PAM, one can obtain scaling laws for how plasma conditions in a particular reactor influence agglomerate growth. For example, the maximum number of primary particles per agglomerate, with an upper limit of 150, is plotted in Fig. 6 as a function of plasma density and electron temperature. With an electron temperature of 1.0 eV, the extent of agglomeration sees a small increase over the range of plasma density of  $1 \times 10^9$  to  $1 \times 10^{11}$   $\text{cm}^{-3}$ . At higher plasma densities, the linearized Debye length is shorter. Therefore, primary particles approaching one end of a large filamentary particle are shielded from the electrostatic repulsion of particles at the far

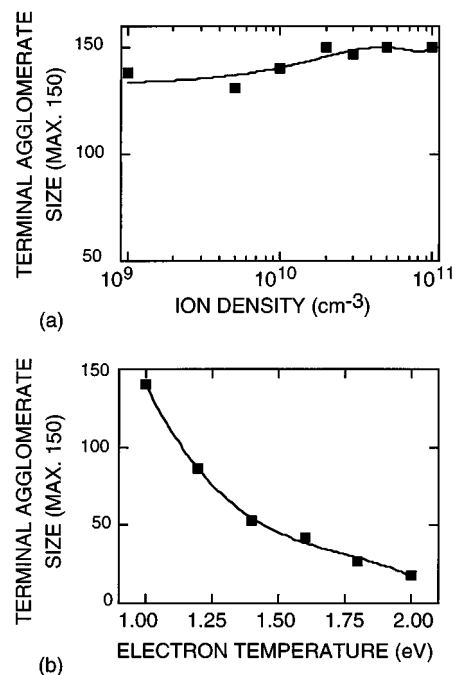


FIG. 6. Maximum agglomerate size while varying (a) ion density and (b) electron temperature. At higher plasma densities, the Debye shielding distance decreases, so that primary particles effectively see less charge on other particles, resulting in a small increase in agglomeration. The surface charge accumulated on primary particles increases with  $T_e$ , increasing the potential barrier for the incoming particle and reducing the amount of agglomeration.

end of the agglomerate to a greater degree at high plasma densities. Since the shielding lengths are commensurate to or larger than the agglomerate size, this effect is not large, and one should see only small increases in agglomerate size with increasing plasma density, as predicted by the MD-PAM.

We see, however, that with increasing electron temperature (plasma density  $1 \times 10^{10}$   $\text{cm}^{-3}$ ), the extent of agglomeration drops significantly. This trend results from the fact that the amount of charge on a primary particle increases with electron temperature, and hence the repulsive potential barrier between particles increases as well. If the kinetic energy of the particles is constant, the value of  $\beta$  decreases, leading to both smaller agglomerates and more filamentary structures.

To demonstrate how reactor conditions can influence agglomeration, particle shapes were computed by the MD-PAM using the velocity distributions shown in Fig. 2 for low and high powered plasmas. Incident particle speeds were randomly chosen from these distributions while having the agglomerate be initially motionless. This simulates the approach of monomer primary particles towards agglomerates trapped at the sheath edge. The resulting agglomerate shapes are shown in Fig. 7 for 100 nm primary particles. The agglomerate generated using the low power velocity distribution is filamentary, reminiscent of particles grown at low  $\beta$ , due to the low cutoff speed of the velocity distribution. The agglomerate generated using the high power velocity distribution is more compact, resembling particles grown at high  $\beta$  due to the influence of the energetic tail of the velocity distribution.

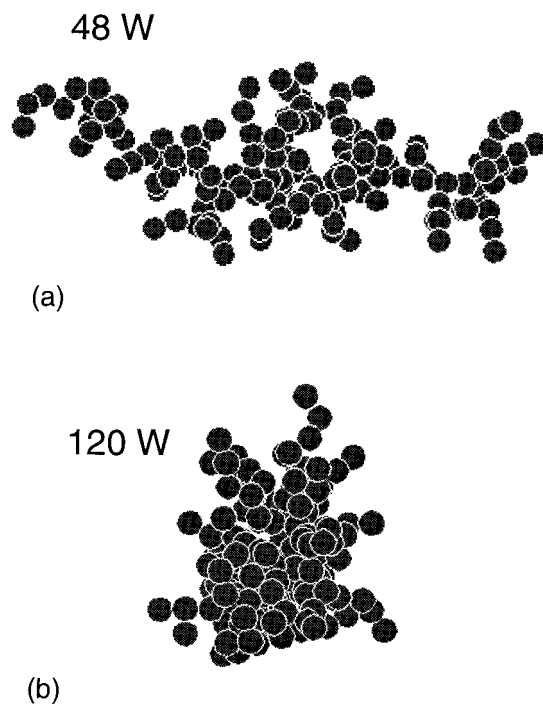


FIG. 7. Agglomerates for 100 nm primary particles produced using the incident velocity distributions from Fig. 2 for (a) lower power and (b) high power plasmas. The agglomerate from the lower powered plasma is filamentary, indicating low  $\beta$ . That for the high power plasma is compact, indicating high  $\beta$ .

#### IV. CONCLUDING REMARKS

We have developed a molecular dynamics simulation as an extension to a particle tracking and agglomeration model for plasma tools with which the shapes of agglomerates can be evaluated. We found that the morphology of dust agglomerates in plasma tools scales with  $\beta \sim R^2 V^2 / T_e^2$ . Larger particles having higher approach velocities in low electron tem-

perature plasmas correspond to large  $\beta$  and tend to form compact agglomerates having high fractal dimensions. These conditions are analogous to the ballistic growth regime for aerosols. Smaller particles having lower approach speeds correspond to small  $\beta$  and tend to form filamentary, low fractal dimension agglomerates. The relative speeds required to form agglomerates in plasmas are 10s to 100s cm/s. These speeds are obtained by dust particles found in the tail of the velocity distributions, usually entering the sheath after having been accelerated by ion drag forces; or after having been injected through gas nozzles.

#### ACKNOWLEDGMENTS

This work was supported by the Semiconductor Research Corporation, Sandia National Laboratories/Sematech, the National Science Foundation (ECS 94-04133 and CTS 94-12565), and the University of Wisconsin ERC for Plasma Aided Manufacturing.

<sup>1</sup>G. S. Selwyn, *Plasma Sources Sci. Technol.* **3**, 340 (1994).

<sup>2</sup>A collection of papers addressing particle transport in plasma processing reactors appears in a Special Issue of *Plasma Sources Sci. Technol.* **3**, 239–451 (1994).

<sup>3</sup>S. J. Choi, P. L. G. Ventzek, R. J. Hoekstra, and M. J. Kushner, *Plasma Sources Sci. Technol.* **3**, 418 (1994).

<sup>4</sup>D. J. Rader and A. S. Geller, *Plasma Sources Sci. Technol.* **3**, 426 (1994).

<sup>5</sup>D. B. Graves, J. E. Daugherty, M. D. Kilgore, and R. K. Porteous, *Plasma Sources Sci. Technol.* **3**, 433 (1994).

<sup>6</sup>J. P. Boeuf, Ph. Belenguer, and T. Hbid, *Plasma Sources Sci. Technol.* **3**, 407 (1994).

<sup>7</sup>P. D. Haaland, A. Garscadden, B. Ganguly, S. Ibrani, and J. Williams, *Plasma Sources Sci. Technol.* **3**, 381 (1994).

<sup>8</sup>W. J. Yoo and Ch. Steinbrüchel, *J. Vac. Sci. Technol. A* **10**, 1041 (1993).

<sup>9</sup>R. N. Carlile, J. F. O'Hanlon, L. M. Hong, M. P. Garrity, and S. M. Collins, *Plasma Sources Sci. Technol.* **3**, 334 (1994).

<sup>10</sup>F. Y. Huang, H. H. Hwang, and M. J. Kushner, *J. Vac. Sci. Technol. A* **14**, 562 (1996).

<sup>11</sup>S. J. Choi and M. J. Kushner, *IEEE Trans. Plasma Sci.* **22**, 138 (1994).

<sup>12</sup>M. D. Kilgore, J. E. Daugherty, R. K. Porteous, and D. B. Graves, *J. Appl. Phys.* **73**, 7195 (1993).

<sup>13</sup>H. H. Hwang and M. J. Kushner, *Appl. Phys. Lett.* **68**, 3716 (1996).

<sup>14</sup>M. Garrity (private communication).